

Article

Inhibition of Carbon Steel Corrosion Using Dextran Derivatives in Circulating Cooling Water

Ping Xu * and Xingrun Chen

Key Laboratory of Urban Stormwater System and Water Environment, Ministry of Education, Beijing University of Civil Engineering and Architecture, Beijing 100044, China; chenxingrun2021@163.com

* Correspondence: xuping@bucea.edu.cn

Abstract: Developing environmentally friendly and biodegradable corrosion inhibitors is an important research direction due to the toxicity and non-degradability of conventional carbon steel corrosion inhibitors added to circulating cooling water environments. Polysaccharides in EPSs (Exopolysaccharides) can be used as green corrosion inhibitors, but a low inhibition rate limits their practical application. Chemical modification is widely used to modify the functionality of polysaccharides by altering their physicochemical properties and structures, thereby enhancing or supplementing their functional characteristics. In this study, we employed chloroacetic acid as an esterifying agent to chemically modify Dextran and successfully synthesized a modified polysaccharide derivative with a substitution degree of 0.326. This derivative efficiently inhibited the corrosion of carbon steel in circulating cooling water environments. The carboxymethylated dextran (CM-Dextran) formed after synthesis could adsorb onto metal surfaces to form a protective film, thereby inhibiting metal surface dissolution reactions and exhibiting anodic corrosion inhibition properties. The experimental results showed that the corrosion inhibition efficiency of CM-Dextran after modification increased by up to 57.4%, with a maximum inhibition efficiency of 82.52% at a concentration of 4 mg/mL. This study provides new insights and opportunities for the development of environmentally friendly corrosion inhibitors derived from polysaccharides.

Keywords: cooling water; carbon steel; green inhibitor; dextran



Citation: Xu, P.; Chen, X. Inhibition of Carbon Steel Corrosion Using Dextran Derivatives in Circulating Cooling Water. *Water* **2024**, *16*, 1182. <https://doi.org/10.3390/w16081182>

Academic Editor: Guangming Jiang

Received: 13 March 2024

Revised: 17 April 2024

Accepted: 19 April 2024

Published: 21 April 2024



Copyright: © 2024 by the authors. Licensee MDPI, Basel, Switzerland. This article is an open access article distributed under the terms and conditions of the Creative Commons Attribution (CC BY) license (<https://creativecommons.org/licenses/by/4.0/>).

1. Introduction

Carbon steel is a common type of steel widely used in circulating cooling water systems [1]. Due to perennial exposure to water, this steel's corrosion resistance is easily compromised [2], and annual losses caused by corrosion account for 2–4% of countries' GDP (Gross Domestic Product) [3], surpassing the combined losses caused by fires, winds, and earthquakes. The presence of Cl^- and SO_4^{2-} in recirculating cooling water environments induces pitting on carbon steel [4] and can penetrate the passive layers of the metal [5], further compromising its corrosion resistance in circulating cooling water environments. Although the addition of corrosion inhibitors in the environment can effectively inhibit the corrosion reaction process [6], traditional corrosion control measures often rely on the use of toxic and dangerous chemicals. Conventional corrosion inhibitors include inorganic and organic types [7], which offer cost-effectiveness, significant efficacy, and ease of use. However, inorganic salt corrosion inhibitors are often resistant to environmental degradation and can pose harm to the environment. Furthermore, by-products produced during the synthesis of organic corrosion inhibitors also present risks to human health and the environment. Additionally, some by-products produced during the synthesis of organic corrosion inhibitors can also pose significant risks to human health and the environment. Currently, there is a shift in corrosion inhibitor research towards emphasizing environmental benefits [8], with scholars increasingly focusing on developing green natural organic extracts as passive corrosion inhibitors [9–12]. Among these inhibitors, Exopolysaccharides (EPSs) are

large sugar molecules (50–50,000 sugar units) produced by a variety of microorganisms, which are secreted in the culture medium [13]. Exopolysaccharides (EPSs) produced by specific bacteria such as sulfate-reducing bacteria [14], desulfurizing bacteria [15], and *Pseudomonas* [16] exhibit environmentally friendly properties and corrosion inhibition capabilities on metals. Research has found that functional groups of polysaccharides, such as carboxyl, play significant roles in inhibiting the corrosion of carbon steel [17]. In addition, different functional group structures can affect the corrosion inhibition effectiveness of polysaccharides as corrosion inhibitors [18]. However, the corrosion inhibition effectiveness of these extracts is unstable, and their inhibitory efficiency is relatively low. Therefore, enhancing the inhibition efficiency of green inhibitors is of paramount importance to promote their application and further development in corrosion inhibition.

Dextran, a microbial polysaccharide, is widely distributed in various fungi and plants and serves as a renewable resource with extensive applications in the food and biomedical sectors [19–21]. Due to the requirements of the sustainable development of the ecological environment, dextran has attracted considerable attention as a green and environmentally friendly corrosion inhibitor [22–24]. However, research indicates that natural polysaccharides have unstable structures, poor solubility, and low inhibition efficiency [25], which limits their further utilization in the field of corrosion inhibitors. Additionally, a large number of hydrogen bonds form within or between polysaccharide molecules. The presence of these bonds inevitably increases the hydrophilicity of dextran [26], leading to a significant decrease in corrosion inhibition efficiency. To overcome these drawbacks, chemical modification methods can be employed to improve the structural characteristics of polysaccharides. Changes in structural and conformational properties can enhance or supplement the functional characteristics of polysaccharides [27]. For example, changes in molecular weight (Mw) and increased solubility typically result in polysaccharides with excellent properties [28] such as superior corrosion inhibition performance [29,30].

In this study, the carboxymethylation of polysaccharides was achieved through nucleophilic substitution reactions, which offer advantages compared to conventional polysaccharide modification methods, such as low reagent consumption, simple operation, safe conversion, and reaction products with low or no toxicity [31]. In the circulating cooling water system, the modified polysaccharide has a stronger ability to adsorb, disperse, and stabilize the liquid phase, which can reduce pollutants and sediments in the water, and prevent the corrosion and scale accumulation of pipelines and equipment, but also improve the efficiency of the system and extend the service life of the equipment, while reducing the impact on the environment [32]. To avoid compromising the green biodegradability of dextran, we drew upon modification methods from the food industry to enhance the corrosion inhibition effectiveness and develop an efficient and environmentally friendly corrosion inhibitor for circulating cooling water, thereby protecting metals from corrosion. Based on the above considerations, we used chloroacetic acid as an esterification agent for the green modification of Dextran and then introduced $-\text{CH}_2\text{COONa}$ between chloroacetic acid and polysaccharides via a bimolecular nucleophilic substitution reaction to prepare carboxymethylated dextran (CM-Dextran) and study it as a green sustainable corrosion inhibitor.

2. Materials and Methods

2.1. Materials

For electrochemical testing, this experiment employed a 20[#] carbon steel electrode with dimensions of 10 mm × 10 mm × 2 mm. One side of the carbon steel electrode served as the working surface, while the other side was connected to a wire. The electrode was encapsulated with epoxy resin, exposing a working area of 1 cm². Weight loss experiments and morphological characterization were conducted using specimens 50 mm × 25 mm × 2 mm in size. The chemical composition of the carbon steel was 0.095 wt% C, 0.170 wt% Si, 0.290 wt% Mn, 0.012 wt% P, and 0.012 wt% S, with Fe constituting the remainder. Before the experiment, both the electrodes and specimens were pretreated, and the metal surfaces

were ground using 180, 360, 600, 800, and 1500 grit dry sand paper with abrasive blades. Then, the polished surface was cleaned with acetone and deionized water, dried with cold air, and placed in a drying dish for 24 h before use. The experiment used recirculating cooling water with a Larson index of 2. The water distribution scheme is shown in Table 1.

Table 1. Composition of the experimental water.

Element	NaCl	Na ₂ SO ₄	NaHCO ₃	pH
(mg/L)	58.5	213	4.2	8.3

2.2. Preparation of a Modified Dextran Corrosion Inhibitor

The preparation method was aqueous method and improved [33]. Figure 1 illustrates the synthesis process for chemically modified polysaccharides, in which Dextran (Sinopharm Chemical Reagent Co., Ltd., Shanghai, China) undergoes a substitution reaction with chloroacetic acid (Aladdin, Astoria, NY, USA). First, 1 g of Dextran was added to 40 mL of isopropanol for stirring, followed by 15 mL of a 20% sodium hydroxide solution. The solution was stirred thoroughly for 1 h until the Dextran was completely dissolved. Then, we slowly added 7 g of chloroacetic acid to achieve the etherification reaction. After the temperature increased to 70 °C and the reaction had continued for 4 h, the pH was adjusted to 7 using a 0.5 mol/mL sodium hydroxide solution. The solution was then placed into a dialysis bag (MV14000), dialyzed with running water for 3 days, and freeze-dried to obtain carboxymethylated Dextran.

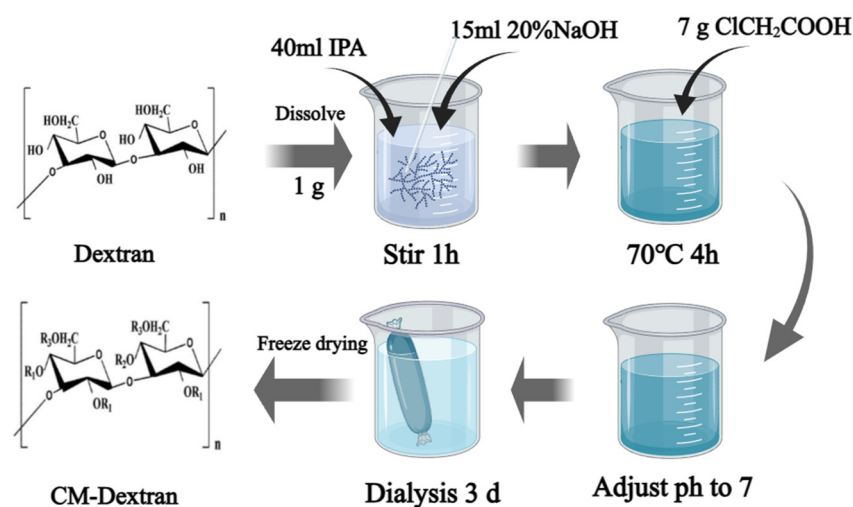


Figure 1. The preparation process for modified polysaccharides.

DS is commonly used to determine the degree of carboxymethyl substitution in hydroxyl groups and is typically measured using acid–base titration [32]. Firstly, a certain amount of HCl solution (0.1 mol/L) was added to a beaker containing 20 mg of CM-Dextran and stirred with a magnetic stirrer at 45 °C for 0.5 h until completely dissolved. After completion, the above solution was titrated with 0.1 mol/L NaOH solution, and the volumes of NaOH solution consumed by the mixed solution at pH 2.1 and pH 4.3 were recorded as V_1 (mL) and V_2 (mL), respectively. The substitution degree of carboxymethylated polysaccharides was then calculated using Equations (1) and (2):

$$A = \frac{[(V_2 - V_1) \times C_{\text{NaOH}}]}{M}, \quad (1)$$

$$DS = \frac{0.023A}{1 - 0.058A}, \quad (2)$$

where A is the carboxymethyl content, C_{NaOH} (mol/L) is the substance concentration, V_1 (mL) is the volume of NaOH solution consumed at pH 2.1, V_2 (mL) is the volume of NaOH solution consumed at pH 4.3, M (g) is the mass of carboxymethylated polysaccharides, and DS is the degree of chemical substitution.

2.3. Experimental Setup

The experiment utilized a self-made AR reactor, as illustrated in Figure 2. This reactor includes a stirring device that simulates the hydraulic flow, a temperature control system, and a water pump for controlling the inlet flow [34]. This device has a volume of 2.5 L and is cylindrical in shape. The outer wall of the reactor, internal rotating shaft, and stirring blades simulating the water flow are composed of organic glass and equipped with racks upon which organic glass test pieces can be placed. During the experiment, the test pieces were placed in a relatively stationary position on the rack. The motor was used to drive the stirring blades, thereby generating shear forces between the water flow and the test piece and simulating the hydraulic conditions in an actual piping network. The speed of the shaft can be adjusted by the controller to simulate the flow rate of water in the recirculating cooling water system. In addition, the reactor is equipped with a heating device to control the water temperature.

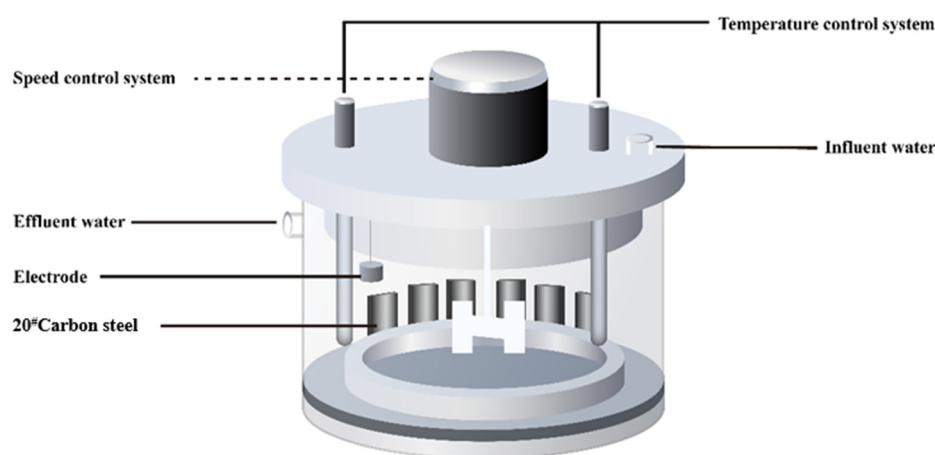


Figure 2. Schematic diagram of the artificial reactor.

We prepared three parallel experiments with a total of nine reactors. Each group contained three operating conditions: the blank condition, polysaccharide condition, and modified polysaccharide condition. Each set included 2 carbon steel electrodes and 6 carbon steel test pieces placed in the reactor, with an experimental rotation speed of 120 r/min and the water temperature controlled at 30 °C. The experiment adopted the non-continuous water inlet method and ran for 10 days.

After the experiment, the carbon steel electrodes and test pieces were removed. Two electrodes were used for electrochemical testing, three test pieces were used for weight loss testing, two test pieces were subjected to scanning electron microscopy (SEM) (QUANTA 200F, The Netherlands) and X-ray photoelectron spectroscopy (XPS) (ULVAC PHI Quantera II, Japan) to detect the surface of the carbon steel, and another test piece was used as a backup.

2.4. Corrosion Weight Loss

Before the experiment, the carbon steel specimens were weighed and immersed for 10 days, as shown in Figure 2. Subsequently, the surface corrosion products were removed using ethanol and deionized water. Simultaneously, a mixture of 10 vol% hydrochloric acid and 5 w/v% hexamethyl-amine was used to clean the remaining corrosion products until complete removal was achieved. The specimens were then dried to a constant weight and weighed using an analytical balance with an accuracy of 0.1 mg. The average weight loss

was obtained from three parallel samples. The corrosion rate and inhibition efficiency were calculated using Equations (3) and (4), respectively:

$$V_{CR}(\text{mma}^{-1}) = \frac{8760 \times \Delta W}{spt} \quad (3)$$

where V_{CR} represents the corrosion rate (mm/a), ΔW is the weight difference of the specimen before and after (g), s is the area of the carbon steel specimen (28 cm²), p is the density (8.4 g/cm³), and t is the immersion time (h).

The inhibition efficiency IR (%) was calculated as follows:

$$IR(\%) = \frac{V_{CR(\text{blank})} - V_{CR(\text{inhibitor})}}{V_{CR(\text{blank})}} \quad (4)$$

where $V_{CR(\text{blank})}$ is the corrosion rate of the blank condition, and $V_{CR(\text{inhibitor})}$ is the corrosion rate after adding Dextran or CM-Dextran to the system.

2.5. Electrochemical Testing

The CHI660C electrochemical workstation (Shanghai, China) with the classic three-electrode system is used for testing and research, which can detect the corrosion of metal materials in the environment [35]. A carbon steel electrode specimen with an area of 1 cm² served as the working electrode, a platinum electrode served as the auxiliary electrode, and a saturated calomel electrode served as the reference electrode. After the system reached a stable state, open circuit potential (OCP) tests were conducted to measure the electrochemical impedance spectroscopy (EIS) and potentiodynamic polarization (PDP) curves. For PDP measurements, a scan range of ± 0.35 V was used at a scan rate of 1 mV/s. For electrochemical impedance spectroscopy, the initial potential was set to the open circuit potential, with a scan frequency of 0.01 to 10⁵ Hz, an amplitude of 0.005, and a settling time of 2 s. ZSimpWin3.60 was employed to fit the impedance spectroscopy data, and the results were analyzed.

2.6. Characterization of the Metal Surface

For scanning electron microscope (SEM) (QUANTA 200F, The Netherlands) with an accelerating voltage range of 200 V to 30 kV and a sample chamber vacuum of $<6 \times 10^{-4}$ –4000 Pa. Before detection, the specimens were coated with platinum to better observe the surface microstructure of the carbon steel without altering its morphology. Additionally, X-ray photoelectron spectroscopy (XPS) and energy-dispersive X-ray spectroscopy (EDS) (ULVAC PHI Quantera II, Japan) were performed to analyze the types of elements present in special structures on the surface. Each XPS spectrum was energy-calibrated using a C 1 s peak as the external standard and the C–C correction position set to 284.8 eV. Fitting and correction were performed using the Avantage v5.9921.

3. Results

3.1. FT-IR Characterization of Dextran Derivatives

Infrared spectroscopy was used to detect the functional groups of Dextran and CM-Dextran, as shown in Figure 3. Although the positions of the infrared absorption peaks of Dextran and CM-Dextran shifted, they were generally similar, indicating that the main structure did not undergo significant changes after modification. Two broad peaks and two narrow peaks were observed around 3402 cm⁻¹, 3432 cm⁻¹, 2936 cm⁻¹, and 2826 cm⁻¹. The absorption peaks around 3600–3200 cm⁻¹ and 3000–2800 cm⁻¹ were characteristic of the -OH and -CH groups in polysaccharides [36]. The absorption peak at 3402 cm⁻¹ in CM-Dextran broadened, indicating enhanced hydrogen bonding due to the introduction of carboxymethyl groups. Additionally, the stretching vibration of the C–H bond at 2936 cm⁻¹ yielded changes in the peak shape and a chemical shift [37]. Compared to Dextran, CM-Dextran exhibited characteristic absorption peaks among the carboxymethyl

groups at 1597 cm^{-1} and 1414 cm^{-1} , representing the stretching vibrations of C=O and -COO, respectively [38].

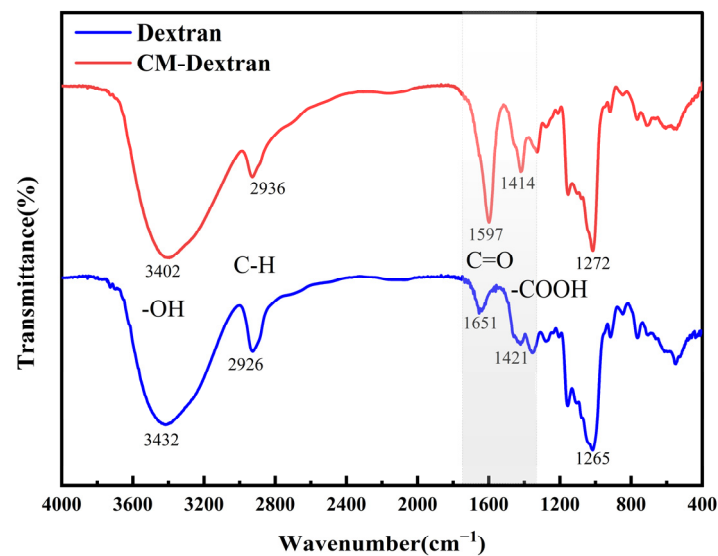


Figure 3. FTIR spectra of Dextran and CM-Dextran.

The above analysis demonstrates that the modification of Dextran was successful. Additionally, the DS of the modified polysaccharide was calculated using acid–base titration to be 0.326. The higher DS of the substitution corresponds to stronger functional properties of the polysaccharide.

3.2. Corrosion Inhibition Properties of CM-Dextran

3.2.1. Corrosion Rate Test

Figure 4 illustrates the variation in the corrosion rate of carbon steel specimens under the simulated circulating cooling water environment. Table 2 presents the inhibition efficiency of Dextran and CM-Dextran at different concentrations.

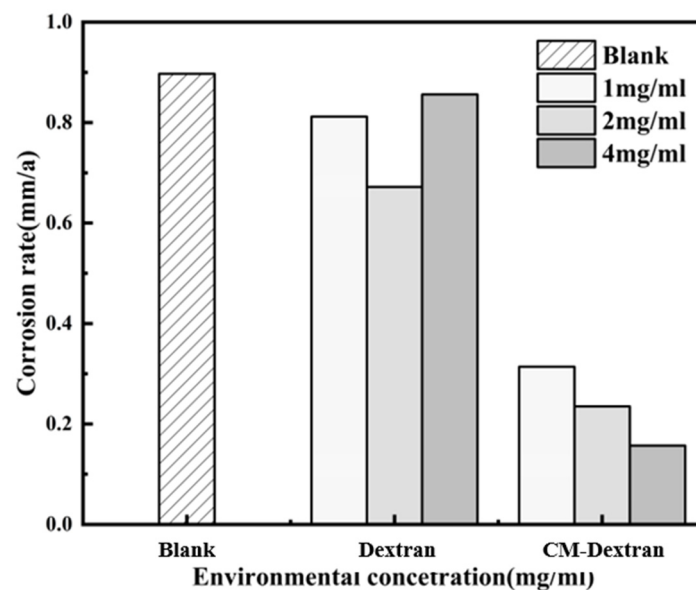


Figure 4. The corrosion rate of the blank and the addition of Dextran and CM-Dextran in circulating cooling water at $30\text{ }^{\circ}\text{C}$.

Table 2. Corrosion rate and corrosion inhibition efficiency based on weight loss method.

Inhibitors	Concentration (mg m·L ⁻¹)	IE (%)
Dextran	1	9.58
	2	25.17
	4	4.68
CM-Dextran	1	65.03
	2	73.83
	4	82.52

Figure 4 and Table 2 indicate that compared to the blank and Dextran conditions, the corrosion rate of carbon steel significantly decreased under the CM-Dextran condition. This result demonstrates the crucial role of CM-Dextran in mitigating the corrosion of carbon steel in circulating cooling water, highlighting the feasibility of CM-Dextran as an efficient corrosion inhibitor. Although Dextran also inhibited corrosion, this effect was not ideal compared to that when using CM-Dextran. Even at a concentration of 2 mg/mL, the highest corrosion inhibition rate was only 25.17%. At concentrations of 1 mg/mL and 4 mg/mL, the corrosion inhibition effect was even poorer at only 9.58% and 4.68%, respectively. This difference is related to the structures of natural polysaccharides. However, after modification, the corrosion resistance of CM-Dextran increased by 57.4%, which is consistent with the results of Luo and Rbaa's research [39,40]. The inhibition effect of CM-Dextran is related to its functional groups [41]. Carboxyl play an important role in the formation of protective layers on the surface of carbon steel [42]. The introduction of carboxymethyl significantly affects the corrosion resistance of Dextran, which may be related to the dense protective layer formed on the surface. Additionally, CM-Dextran's effectiveness in inhibiting corrosion showed a positive correlation with its concentration. For instance, when the concentration was 1 mg/mL, the corrosion rate of the carbon steel was 0.314 mm/a. However, as the concentration increased to 4 mg/mL, the corrosion rate of the carbon steel decreased significantly to 0.157 mm/a. The inhibition efficiency peaked at this juncture, reaching 82.52% compared to the blank. This observation suggests that despite varying concentration conditions, the fluctuation in inhibition efficiency remained within approximately 10%. Therefore, even when consumed in the environment, CM-Dextran maintained a stable corrosion inhibition effect on the carbon steel. Research indicates that the structure of CM-Dextran is more stable [43]. Table 3 shows that CM-Dextran differs from Dextran only in its functional groups, indicating that CM-Dextran still possesses green biodegradability characteristics. In this experiment, CM-Dextran demonstrated persistent corrosion inhibition performance in the circulating cooling water system, helping to overcome the easy failure of green corrosion inhibitors after long-term use with high efficiency and stability.

Table 3. Polarization parameters of Dextran and CM-Dextran at different concentrations in circulating cooling water at 30 °C.

Inhibitors	Concentration (mg m·L ⁻¹)	E _{corr} (V)	I _{corr} /mA/cm ²	βa/mV·dec ⁻¹	−βc/mV·dec ⁻¹
Dextran	1	−0.648	0.03259	207	185
	2	−0.682	0.02882	213	185
	4	−0.658	0.03753	209	166
CM-Dextran	1	−0.571	0.02351	238	181
	2	−0.542	0.02401	255	175
	4	−0.498	0.01980	397	133

3.2.2. Electrochemical Measurements

To further investigate the electrochemical reaction process of CM-Dextran on the surface of carbon steel, potentiodynamic polarization (PDP) and electrochemical impedance spectroscopy (EIS) experiments were conducted to study the corrosion inhibition behavior of CM-Dextran under simulated circulating cooling water environments. Figure 5 illustrates the polarization curves of carbon steel electrodes after exposure to different concentrations of Dextran and CM-Dextran in the environment. Table 3 presents the parameters obtained after Tafel fitting.

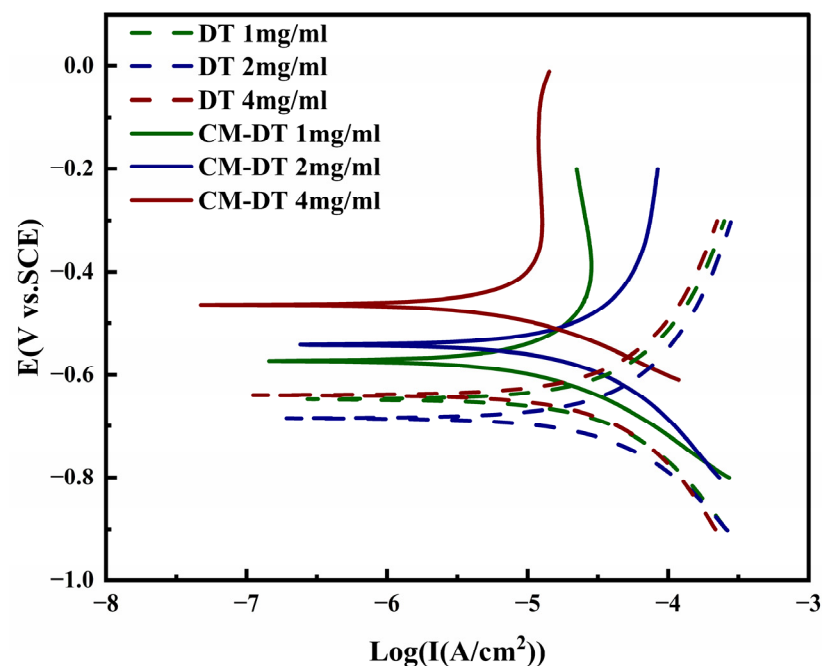


Figure 5. The electrochemical curve of Dextran and CM-Dextran at different concentrations in circulating cooling water at 30 °C.

Figure 5 and Table 3 show a positive shift in the corrosion potential under the CM-Dextran condition compared to that under the Dextran condition. The corrosion potential ranges for the two conditions were -0.682 to -0.658 V and -0.498 to -0.571 V, respectively, indicating the reduced corrosion tendency of carbon steel under the CM-Dextran condition. At a concentration of 4 mg/mL, there was a significant positive shift of 0.160 V, indicating the weakest corrosion tendency. The corrosion current density showed similar results, with the lowest corrosion current densities being 0.01980 mA/cm² and 0.02882 mA/cm² for the two conditions, respectively, representing a decrease of approximately 45.56%. The corrosion potential and current density results indicate that carbon steel offers good corrosion resistance in environments containing CM-Dextran, which is consistent with the corrosion weight loss results shown in Figure 4. Overall, these results indicate improved corrosion inhibition performance after Dextran modification.

The Tafel slope parameters in Table 3 show that the anodic slope β_a was higher than the cathodic slope β_c for both CM-Dextran and Dextran, indicating that the anodic reaction was the controlling factor under both conditions. In the anodic region, iron undergoes oxidation, producing iron ions and electrons, as follows: $\text{Fe} \rightarrow \text{Fe}^{2+} + 2e^-$. In the cathodic region, oxygen undergoes reduction, accepting electrons and reacting with water to form hydroxide ions: $1/2\text{O}_2 + \text{H}_2\text{O} + 2e^- \rightarrow 2\text{OH}^-$. The hydroxide ions then combine with iron ions to form water while also generating iron hydroxide or hydrated iron oxide: $2\text{Fe}^{2+} + 4\text{OH}^- \rightarrow \text{Fe}_2(\text{OH})_4 \downarrow$. However, under the CM-Dextran condition, the anodic slope β_a increased by 31 mV·dec⁻¹ to 188 mV·dec⁻¹ compared to the slope under the Dextran condition, indicating an enhanced control of the anodic reaction after modification. With

an increase in concentration, the anodic slope β_a of CM-Dextran increased, indicating a weakening of the electron-donating ability of Fe on the carbon steel surface and suppressing metal corrosion. The changes in the values of β_a and β_c for Dextran were not significant. However, when the concentration of CM-Dextran reached 4 mg/mL, β_a increased by $159 \text{ mV}\cdot\text{dec}^{-1}$ while β_c decreased by $133 \text{ mV}\cdot\text{dec}^{-1}$. We argue that CM-Dextran inhibits the anodic dissolution reaction of iron. Then, CM-Dextran modified with carboxymethyl groups undergoes adsorption complexation on the surface of the carbon steel, forming a protective layer [44]. Additionally, after surface adsorption, CM-Dextran enhances the reduction ability of Fe [45], thereby reducing the number of electrons lost by Fe and weakening the anodic dissolution reaction of the metal. The process by which CM-Dextran inhibits carbon steel corrosion exhibits the characteristics of anodic inhibitors.

Figure 6 displays the Nyquist and Bode plots of carbon steel electrodes after the addition of Dextran and CM-Dextran into the environment. The Nyquist plots exhibit a complete semicircle in the high-frequency region and an incomplete semicircle in the low-frequency region. Additionally, the Bode plot shows the presence of two distinct constant phase angles after the addition of CM-Dextran. These angles are related to the formation of inhibitor protective films [46] and charge transfer. Generally, the larger the diameter of the Nyquist semicircle, the lower the corrosion rate [47]. The fitted circuit conformed to the $R_s(Q_b(R_b(Q_fR_p)))$ model, with the equivalent circuits illustrated in Figure 7. The circuit consists of a constant phase element (Q_b) and resistance (R_b) in parallel with double-layer capacitance (Q_f) and charge transfer resistance (R_p), while 'n' represents the diffusion coefficient. Throughout the Nyquist evaluation process, R_s represents the solution resistance; R_b and R_p , respectively, represent the membrane resistance (corrosion products on the metal surface) and interfacial charge transfer resistance; and R_s , R_b , and R_p together constitute the charge transfer resistance.

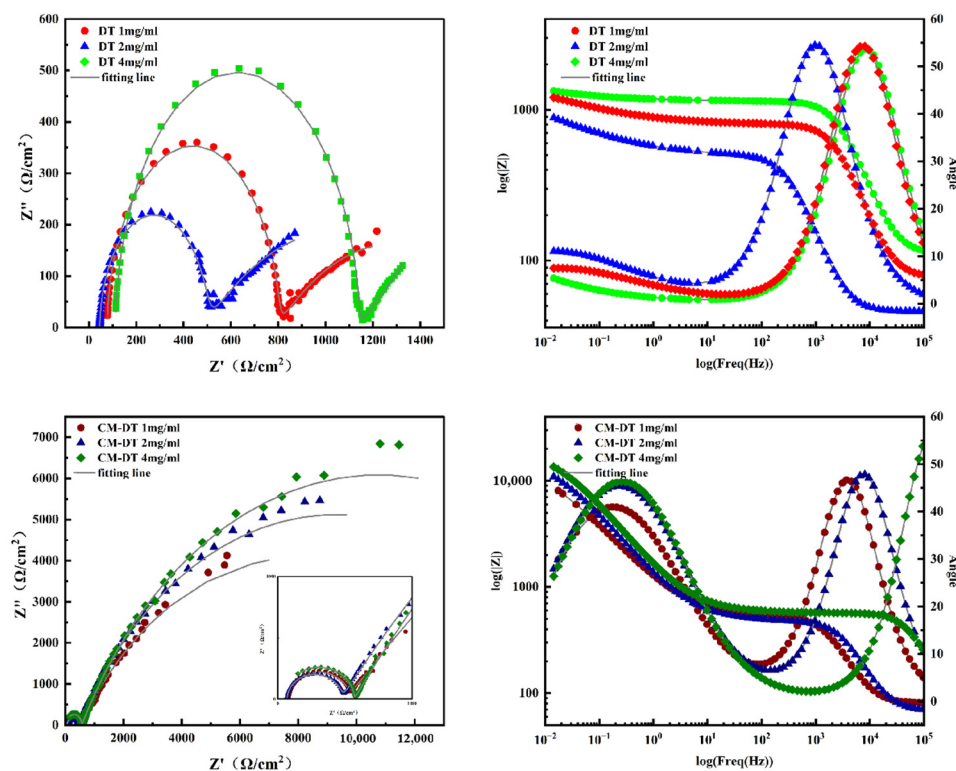


Figure 6. Nyquist and Bode plots of Dextran and CM-Dextran at different concentrations in circulating cooling water at 30 °C.

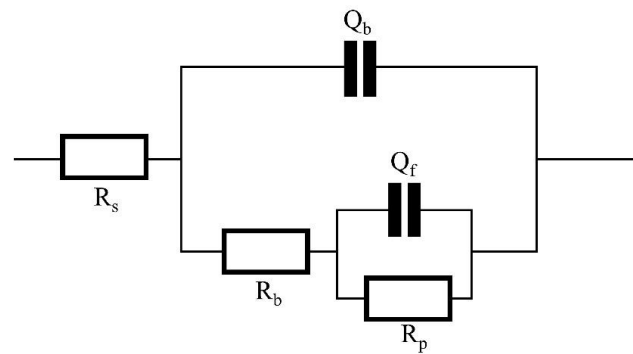


Figure 7. The equivalent circuit diagram for carbon steel.

As shown in Figure 6 and Table 4, the relationship between R_b and R_p differed between the Dextran and CM-Dextran conditions. The ranges of R_b and R_p under the Dextran condition were $718 \Omega \cdot \text{cm}^2$ to $1027 \Omega \cdot \text{cm}^2$ and $993 \Omega \cdot \text{cm}^2$ to $1626 \Omega \cdot \text{cm}^2$, respectively, with a small difference between the two that jointly affected the corrosion of the carbon steel. However, under the CM-Dextran condition, the ranges of R_b and R_p were $406 \Omega \cdot \text{cm}^2$ to $450 \Omega \cdot \text{cm}^2$ and $11,130 \Omega \cdot \text{cm}^2$ to $17,650 \Omega \cdot \text{cm}^2$, respectively. R_p was an order of magnitude higher than R_b , indicating that R_p offered the main resistance to corrosion on the surface of the carbon steel at this time, with ranges more than 10 times higher than those before modification, indicating a significant decrease in the charge transfer capability of the carbon steel surface after modification. This result also explains the significant decrease in corrosion rate, the positive shift in corrosion potential, and the decrease in corrosion current density, as shown in Figure 4 and Table 3. The protective film on the surface of the carbon steel was composed of an inhibitor film adsorbed by CM-Dextran and generated corrosion products, which play an important role in protecting carbon steel [48,49]. However, after modification, CM-Dextran acquired the characteristics of anodic inhibitors due to its excellent corrosion resistance, thereby weakening the oxidation reaction on the surface of the carbon steel and slowing the generation of corrosion products (see Table 3). In addition, the 'n' value indicates the uniformity of the surface of carbon steel with CM-Dextran and Dextran. The diffusion coefficient n_f was >0.5 under the CM-Dextran condition, while n_f was <0.5 under the Dextran condition, indicating that the surface of the modified carbon steel was more uniform.

Table 4. Electrochemical impedance parameters of Dextran and CM-Dextran at different concentrations in circulating cooling water at 30 °C.

Inhibitors	Concentration (mg/mL)	$R_s/\Omega \cdot \text{cm}^2$	n_b	$R_b/\Omega \cdot \text{cm}^2$	n_f	$R_p/\Omega \cdot \text{cm}^2$
Dextran	1	77	0.98	718	0.406	993
	2	108	0.98	997	0.444	1626
	4	110	0.97	1027	0.366	1358
CM-Dextran	1	80	0.98	450	0.662	11,130
	2	101	0.99	406	0.654	14,650
	4	68	0.99	404	0.669	17,650

The PDP and EIS results show that CM-Dextran had an impact on the electrochemical reaction process at the interface of the carbon steel. The improvement in inhibition efficiency after modification was closely related to the protective layer on the surface of the carbon steel.

3.3. SEM Analysis of the Carbon Steel Surface

To further investigate the protective film formed by CM-Dextran on the surface of the carbon steel, we conducted a high-resolution SEM-EDS analysis of the steel's corrosion

interface. Figures 8 and 9, respectively, present the surface morphology and EDS detection results under three different conditions. According to the SEM results, there were significant differences in the surface morphology of carbon steel under different conditions.

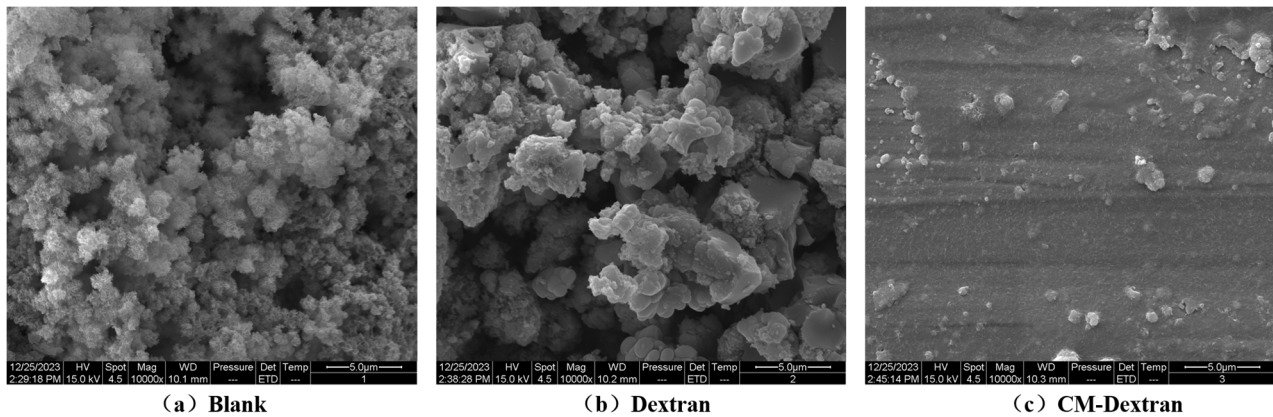


Figure 8. SEM of carbon surface under circulating cooling water at 30 °C.

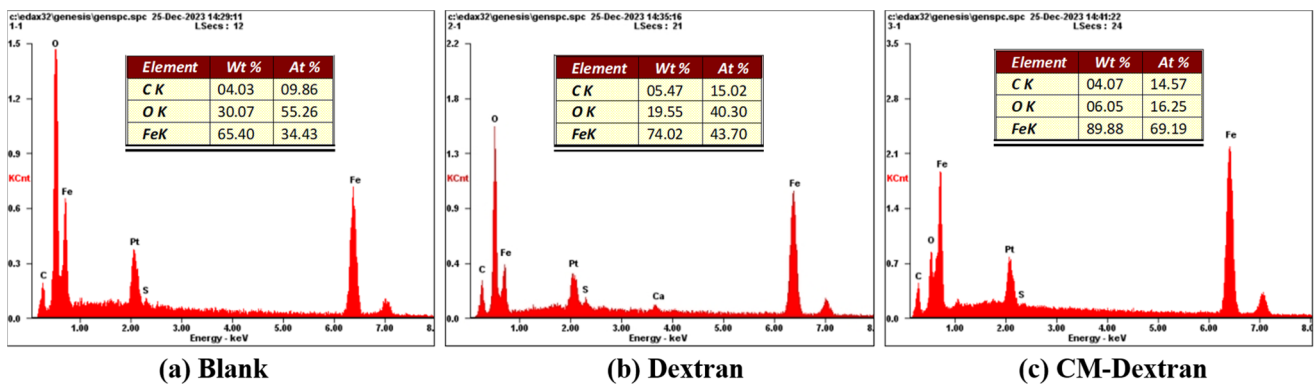


Figure 9. EDS of carbon surface under circulating cooling water at 30 °C.

Based on the results shown in Figures 8 and 9, the surface of the carbon steel was extremely rough and exhibited a porous structure under both the blank and Dextran conditions, with noticeable spherical corrosion products. However, despite the presence of some white granular substances, the surface of the carbon steel was very uniform after modification, with fewer corrosion products; the film structure was also smoother. This result is consistent with the reduction in R_f and increase in the diffusion coefficient n , as indicated in Table 4. Additionally, the localized EDS detection results show that the surface under all three conditions contained the same elements: O, Fe, and C. In both the CM-Dextran and Dextran conditions, there was a decrease in the O element of approximately 39.01% and 24.05%, respectively, further demonstrating CM-Dextran's inhibition of the Fe oxidation reaction on the carbon steel surface. In this way, CM-Dextran acts as an anodic corrosion inhibitor, effectively suppressing corrosion reactions on the surface of the carbon steel. In addition to adsorbing onto the metal surface to form a dense protective layer and isolating corrosive ions, CM-Dextran also has a scavenging effect on strong oxidizing free radicals in aqueous solutions [50,51], reducing the probability of iron oxidation. Thus, CM-Dextran exhibits highly efficient corrosion inhibition effects on carbon steel from the perspective of both the carbon steel interface and the corrosive environment medium.

3.4. Analysis of CM-Dextran's Adsorption Mechanism

The SEM analysis indicates that the corrosion inhibition effect of CM-Dextran is primarily attributable to its adsorption onto the surface of carbon steel, enabling it to form a dense protective film. To further investigate the adsorption protection mechanism, we

studied the adsorption film-forming properties of CM-Dextran on the surface of carbon steel through adsorption isotherms, as shown in Figure 10. In this study, the Langmuir equation was employed to fit the adsorption isotherms. This method is commonly used to study the adsorption of environmentally friendly corrosion inhibitors on metal surfaces [52].

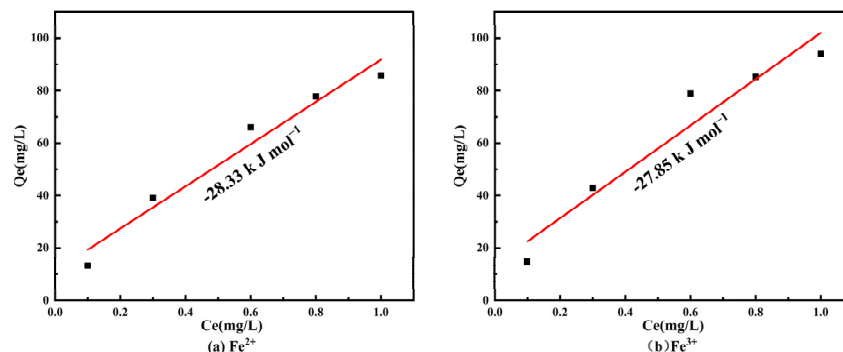


Figure 10. The Langmuir adsorption isotherm of CM-Dextran on $\text{Fe}^{2+}/\text{Fe}^{3+}$ adsorption in circulating cooling water at 30 °C.

The Langmuir isotherm equation is

$$\frac{C_e}{Q_e} = \frac{1}{bQ_m} + \frac{C_e}{Q_m}, \quad (5)$$

where C_e is the equilibrium concentration of $\text{Fe}^{2+}/\text{Fe}^{3+}$, Q_e is the adsorption amount of $\text{Fe}^{2+}/\text{Fe}^{3+}$, Q_m is the saturation adsorption capacity of the adsorbent (mg/g), and b is the equilibrium adsorption coefficient.

The relationship between the equilibrium adsorption constant b and the Gibbs free energy ΔG can be calculated using the following formula:

$$\Delta G = -RT \ln(55.56b) \quad (6)$$

where ΔG is the Gibbs free energy change, R is the gas constant (typically 8.314 J/(mol·K)), T is the temperature in Kelvin, and b is the equilibrium adsorption constant.

Table 5 presents the thermodynamic adsorption parameters of CM-Dextran fitted using the Langmuir equation. Table 5 shows that the R^2 values are all 0.99, indicating that the Langmuir equation can accurately describe the adsorption process of CM-Dextran on $\text{Fe}^{2+}/\text{Fe}^{3+}$. The results for CM-Dextran's maximum $\text{Fe}^{2+}/\text{Fe}^{3+}$ adsorption capacity (Q_m) suggest that the adsorption capacity for Fe^{3+} is greater than that for Fe^{2+} . Adsorption processes are generally classified into physical adsorption and chemical adsorption. Physical adsorption is mainly caused by van der Waals forces, with electrostatic adsorption being the most common form. Negatively charged functional groups in polysaccharides electrostatically adsorb to positively charged metal ions, whereas chemical adsorption primarily occurs through the complexation of functional groups via covalent bonds with metals. ΔG is commonly used to evaluate the adsorption properties of corrosion inhibitors on metals. The ΔG values for $\text{Fe}^{2+}/\text{Fe}^{3+}$ shown in Table 5 are all negative, indicating that the adsorption process of CM-Dextran on the surface of carbon steel is spontaneous. A ΔG value higher than -20 kJ mol^{-1} indicates physical adsorption of the inhibitor on the metal [53], while a ΔG value lower than -40 kJ mol^{-1} indicates chemical adsorption [54]. Values between these two thresholds indicate mixed physical/chemical adsorption. The ΔG values for $\text{Fe}^{2+}/\text{Fe}^{3+}$ were $-28.33 \text{ kJ mol}^{-1}$ and $-27.85 \text{ kJ mol}^{-1}$, respectively, and were thus positioned between the two thresholds. This result suggests that the adsorption process of CM-Dextran involves both physical and chemical adsorption processes. Chemical adsorption is generally considered more stable than physical adsorption. In addition, the formation of metal complexes through chemical adsorption by CM-Dextran played a significant role in the densification of the protective film.

Table 5. The thermodynamic adsorption parameters of CM-Dextran on Fe²⁺/Fe³⁺ adsorption in circulating cooling water at 30 °C.

Condition	R ²	Q _m (mg/L)	b (mg/L)	ΔG (kJ mol ⁻¹)
Fe ²⁺	0.99	65.24	1.38	−28.33
Fe ³⁺	0.99	155.04	1.14	−27.85

To further investigate the adsorption and protection mechanism of CM-Dextran, we conducted an XPS analysis to examine the functional groups and corrosion products adsorbed on the surface of the carbon steel samples. Figure 11 presents the high-resolution XPS spectra for the total spectrum, C 1 s, O 1 s, and Fe2p3/2, along with the binding energies of each peak component.

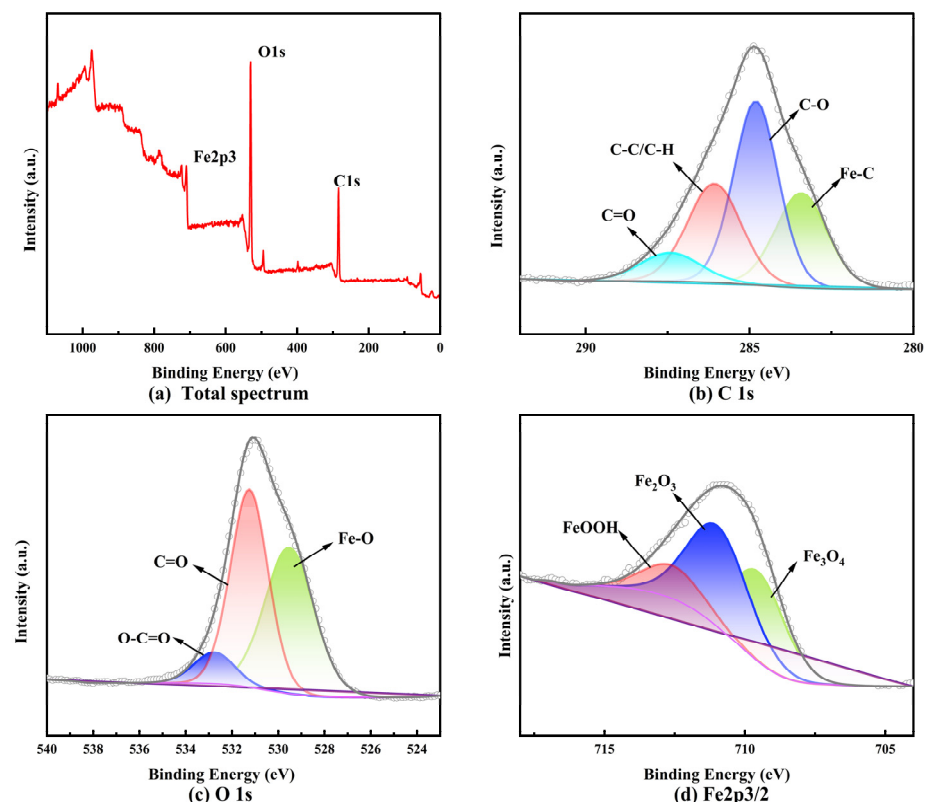
**Figure 11.** XPS spectra for corrosion products formed in circulating cooling water at 30 °C containing 2 mg/mL CM-Dextran.

Figure 11b and Figure 11c, respectively, represent the C 1 s spectrum and O 1 s spectrum. In the C 1 s spectrum, there are four convolution peaks at 283.42 eV, 284.8 eV, 287.07 eV, and 287.71 eV, representing Fe–C, C–C/C–H, C–O, and C=O, with relative atomic percentages of 24.13%, 40.6%, 26.52%, and 8.76%, respectively. This result indicates that CM-Dextran adsorption on the carbon steel surface involves the strong physical adsorption of C–O and C=O, which played an important role in forming the protective film on the carbon steel surface [55]. Here, C–C/C–H had the highest content on the carbon steel surface. The modification introducing carboxyl methyl enhanced the film-forming effect of CM-Dextran on the carbon steel. The results for Fe–C further indicate that CM-Dextran underwent coordination reactions with Fe in the solution, demonstrating that CM-Dextran exhibits not only physical adsorption but also chemical adsorption, consistent with the thermodynamic parameters obtained from the Langmuir equation fitting presented in Table 5. The O 1 s spectrum in Figure 11b shows three convolution peaks at 529.56 eV, 531 eV, and 532.76 eV, corresponding to Fe–O, C=O, and O–C=O, respectively, with relative

atomic contents of 45.03%, 46.89%, and 8.07%. The high content of Fe-O and C=O indicates a significant adsorption of metal corrosion products and CM-Dextran on the surface. The lowest content of O-C=O may be related to complexation with Fe deposited in the interior.

Figure 11d presents the Fe2p3/2 spectrum, which can be deconvoluted into three peaks at 709.54 eV, 710.97 eV, and 712.56 eV, corresponding to Fe₃O₄, Fe₂O₃, and FeOOH, with Fe²⁺ and Fe³⁺ contents of 70.81% and 29.19%, respectively. The surface of the carbon steel contained more Fe²⁺, while the formation of Fe³⁺ was often related to further oxidation of Fe²⁺. CM-Dextran adsorption on the surface inhibited the oxidation reaction of the metal surface. Additionally, the formed corrosion inhibition film hindered the dissolution of Fe, enriching Fe²⁺ on the metal surface. Moreover, CM-Dextran promoted the reduction of Fe and inhibited the corrosion of carbon steel, consistent with the conclusions in Table 3.

4. Discussion

Based on the results of electrochemical, SEM, and CM-Dextran adsorption mechanism analyses, CM-Dextran provides corrosion protection to carbon steel mainly via adsorption and film formation [56], thereby inhibiting anodic dissolution. Figure 12 illustrates the mechanism by which CM-Dextran inhibits carbon steel corrosion in the environment. Following modification, CM-Dextran contained more functional groups. Due to corrosion, the emergence of adsorption sites resulted in the physical adsorption of C-C/C-H, C-O, C=O, and O-C=O onto the surface of the carbon steel. Negatively charged groups underwent electrostatic adsorption with positively charged metals, forming a protective film, which effectively slowed the dissolution of metals [1]. Furthermore, CM-Dextran underwent chemical adsorption with Fe²⁺/Fe³⁺ to form stable covalent bonds, thereby generating metal complexes and establishing specific permanent adsorption. Additionally, gradual aggregation into a film occurred through particle interactions and solid-state reactions, including intermolecular forces such as hydrogen bonds and electrostatic interactions, covering the dense protective film composed of CM-Dextran. This protective film inhibited Fe dissolution and blocked corrosion ion erosion. Furthermore, CM-Dextran enhanced the reduction capability of iron, weakening its electron transfer ability and significantly reducing the charge transfer on the metal surface. These processes enhanced charge transfer resistance and protected the carbon steel substrate.

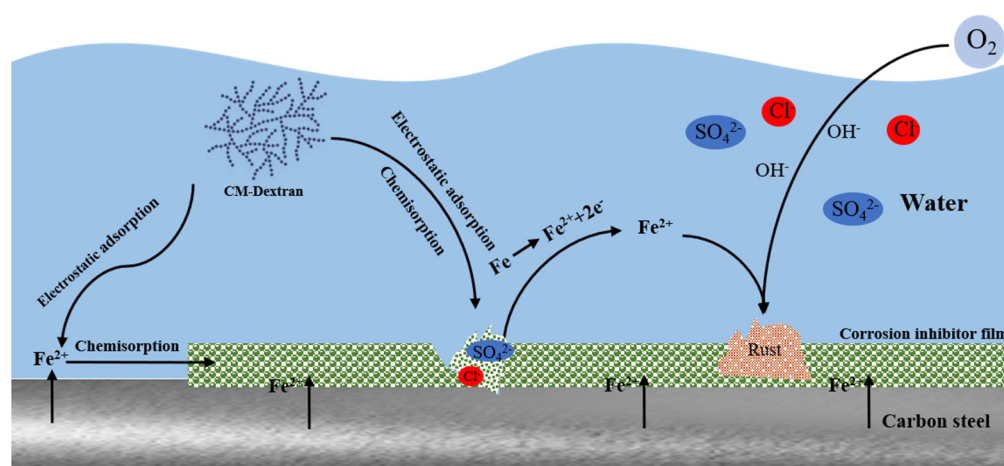


Figure 12. Mechanism for inhibiting the corrosion of carbon steel.

5. Conclusions

This study successfully prepared modified Dextran, i.e., CM-Dextran, and applied it as a green, environmentally friendly, and novel corrosion inhibitor in circulating cooling water for carbon steel. This green, biodegradable polysaccharide structure offers a new approach and opportunity for the development of corrosion inhibitors. Through comprehensive analyses, we drew the following conclusions:

- (1) Dextran and CM-Dextran are green and environmentally friendly corrosion inhibitors that offer excellent capabilities in inhibiting carbon steel corrosion. In this study, Dextran yielded a corrosion inhibition rate of 25.17% at 2 mg/mL, while CM-Dextran achieved the highest corrosion inhibition rate of 82.52% at 4 mg/mL. Chemical modification did not compromise the green characteristics of the carbon steel. Dextran exhibited low and unstable inhibition efficiency, while modified CM-Dextran enhanced the corrosion inhibition capability by 57.35% and demonstrated long-term stability, thus overcoming natural green corrosion inhibitors' susceptibility to degradation.
- (2) The results of electrochemical kinetics testing indicated that after the addition of CM-Dextran, the corrosion potential range of the carbon steel was between -0.498 and -0.571 V. Compared to the results with the addition of Dextran, the corrosion tendency of carbon steel decreased, and the corrosion current density decreased. β_a was greater than β_c , indicating anodic corrosion inhibition capacity. When the environmental concentration reached 4 mg/mL, β_a increased by $159 \text{ mV}\cdot\text{dec}^{-1}$, effectively inhibiting the metal dissolution reaction on the surface of the carbon steel. Electrochemical impedance spectroscopy and SEM demonstrated that CM-Dextran formed a smooth protective film on the surface of the carbon steel. This film structure impeded the metal dissolution reaction on the surface of the carbon steel, resulting in a 14.96% decrease in surface oxygen content.
- (3) CM-Dextran adsorbed $\text{Fe}^{2+}/\text{Fe}^{3+}$ with ΔG values of $-28.33 \text{ kJ mol}^{-1}$ and $-27.85 \text{ kJ mol}^{-1}$, involving both physical and chemical adsorption processes. XPS testing revealed that CM-Dextran adsorbed onto the C–C/C–H, C–O, and C=O sites on the surface of the carbon steel. The surface content of Fe^{2+} and Fe^{3+} was 70.81% and 29.19%, respectively, with electrostatic adsorption occurring between $\text{Fe}^{2+}/\text{Fe}^{3+}$ and CM-Dextran. Additionally, metal complexes were formed through covalent bonds. These complexes covered the metal surface to form a dense protective film, effectively inhibiting the corrosion process of the carbon steel.

Author Contributions: P.X.: conceptualization, supervision, project administration, review and editing, validation, and funding acquisition. X.C.: data curation, methodology, investigation, data analysis, visualization, original draft preparation, and draft modification. All authors have read and agreed to the published version of the manuscript.

Funding: This study was supported by the National Natural Science Foundation of China (No. 51578035) and the National Major Water Pollution and Treatment Project of China (No. 2018ZX07110-008-006).

Data Availability Statement: The data presented in this study are available on request from the corresponding author. The data are not publicly available due to privacy.

Conflicts of Interest: The authors declare no conflicts of interest.

References

1. Branzoi, F.; Branzoi, V.; Licu, C. Corrosion inhibition of carbon steel in cooling water systems by new organic polymers as green inhibitors. *Mater. Corros.* **2014**, *65*, 637–647. [[CrossRef](#)]
2. Seo, B.; Kanematsu, H.; Nakamoto, M.; Miyabayashi, Y.; Tanaka, T. Corrosion resistance and antibacterial activity of a surface coating created by super-spread wetting of liquid copper on laser-ablated carbon steel. *Surf. Coat. Technol.* **2022**, *445*, 128706. [[CrossRef](#)]
3. Kokilaramani, S.; Al-Ansari, M.M.; Rajasekar, A.; Al-Khattaf, F.S.; Hussain, A.; Govarthanan, M. Microbial influenced corrosion of processing industry by re-circulating waste water and its control measures—A review. *Chemosphere* **2021**, *265*, 129075. [[CrossRef](#)] [[PubMed](#)]
4. Deyab, M. The influence of different variables on the electrochemical behavior of mild steel in circulating cooling water containing aggressive anionic species. *J. Solid State Electrochem.* **2009**, *13*, 1737–1742. [[CrossRef](#)]
5. Deyab, M. Electrochemical investigations on pitting corrosion inhibition of mild steel by provitamin B5 in circulating cooling water. *Electrochim. Acta* **2016**, *202*, 262–268. [[CrossRef](#)]
6. Chauhan, D.S.; Sorour, A.A.; Saji, V.S.; Quraishi, M.A. Green corrosion inhibitors based on biomacromolecules and macrocycles: A review. *Sustain. Chem. Pharm.* **2023**, *36*, 101295. [[CrossRef](#)]
7. Al-Amiery, A.; Wan Isahak, W.N.R.; Al-Azzawi, W.K. Sustainable corrosion Inhibitors: A key step towards environmentally responsible corrosion control. *Ain Shams Eng. J.* **2024**, *15*, 102672. [[CrossRef](#)]

8. Medupin, R.O.; Ukoba, K.O.; Yoro, K.O.; Jen, T.-C. Sustainable approach for corrosion control in mild steel using plant-based inhibitors: A review. *Mater. Today Sustain.* **2023**, *22*, 100373. [[CrossRef](#)]
9. Gerengi, H.; Schaefer, K.; Sahin, H.I. Corrosion-inhibiting effect of Mimosa extract on brass-MM55 corrosion in 0.5 M H₂SO₄ acidic media. *J. Ind. Eng. Chem.* **2012**, *18*, 2204–2210. [[CrossRef](#)]
10. Wang, Q.; Zhang, Q.; Zhao, C.; Wang, R.; Zhou, X.; Sun, Y.; Yan, Z.; Li, X. Study on the corrosion inhibitory performance of Pomacea canaliculata extract as a corrosion inhibitor for carbon steel in acidic environments. *J. Mol. Liq.* **2024**, *394*, 123754. [[CrossRef](#)]
11. Wang, Q.; Zheng, H.; Liu, L.; Zhang, Q.; Wu, X.; Yan, Z.; Sun, Y.; Li, X. Insight into the anti-corrosion behavior of Reineckia Carnea leaves extract as an eco-friendly and high-efficiency corrosion inhibitor. *Ind. Crops Prod.* **2022**, *188*, 115640. [[CrossRef](#)]
12. Mohammadi, Z.; Rahsepar, M. The use of green Bistorta Officinalis extract for effective inhibition of corrosion and scale formation problems in cooling water system. *J. Alloys Compd.* **2019**, *770*, 669–678. [[CrossRef](#)]
13. van Hijum, S.A.; Kralj, S.; Ozimek, L.K.; Dijkhuizen, L.; van Geel-Schutten, I.G. Structure-function relationships of glucansucrase and fructansucrase enzymes from lactic acid bacteria. *Microbiol. Mol. Biol. Rev.* **2006**, *70*, 157–176. [[CrossRef](#)]
14. Dong, Z.H.; Liu, T.; Liu, H.F. Influence of EPS isolated from thermophilic sulphate-reducing bacteria on carbon steel corrosion. *Biofouling* **2011**, *27*, 487–495. [[CrossRef](#)] [[PubMed](#)]
15. Fu, M.; Cheng, X.; Li, J.; Chen, S.; Dou, W.; Liu, G. Influence of soluble, loosely bound and tightly bound extracellular polymeric substances (EPS) produced by Desulfovibrio vulgaris on EH40 steel corrosion. *Corros. Sci.* **2023**, *221*, 111342. [[CrossRef](#)]
16. Bautista, B.E.T.; Wikieł, A.J.; Datsenko, I.; Vera, M.; Sand, W.; Seyeux, A.; Zanna, S.; Frateur, I.; Marcus, P. Influence of extracellular polymeric substances (EPS) from Pseudomonas NCIMB 2021 on the corrosion behaviour of 70Cu–30Ni alloy in seawater. *J. Electroanal. Chem.* **2015**, *737*, 184–197. [[CrossRef](#)]
17. Ghafari, M.D.; Bahrami, A.; Rasooli, I.; Arabian, D.; Ghafari, F. Bacterial exopolymeric inhibition of carbon steel corrosion. *Int. Biodeterior. Biodegrad.* **2013**, *80*, 29–33. [[CrossRef](#)]
18. Umoren, S.A.; Solomon, M.M.; Saji, V.S. (Eds.) Chapter 5—Chitosan. In *Polymeric Materials in Corrosion Inhibition*; Elsevier: Amsterdam, The Netherlands, 2022; pp. 131–153.
19. Lazić, V.; Vivod, V.; Peršin, Z.; Stoiljković, M.; Ratnayake, I.S.; Ahrenkiel, P.S.; Nedeljković, J.M.; Kokol, V. Dextran-coated silver nanoparticles for improved barrier and controlled antimicrobial properties of nanocellulose films used in food packaging. *Food Packag. Shelf Life* **2020**, *26*, 100575. [[CrossRef](#)]
20. Chen, Z.; Chen, J.; Ni, D.; Xu, W.; Zhang, W.; Mu, W. Microbial dextran-hydrolyzing enzyme: Properties, structural features, and versatile applications. *Food Chem.* **2024**, *437*, 137951. [[CrossRef](#)]
21. Yao, J.; Jiang, Y.; Dong, H.; Li, A. Nano-encapsulation of EGCG in dextran 70-stabilized chitosan/SDS nanoparticles: Characterization, permeability behavior and oral bioavailability. *Eur. Polym. J.* **2024**, *205*, 112763. [[CrossRef](#)]
22. Luo, X.; Pan, X.; Yuan, S.; Du, S.; Zhang, C.; Liu, Y. Corrosion inhibition of mild steel in simulated seawater solution by a green eco-friendly mixture of glucomannan (GL) and bisquaternary ammonium salt (BQAS). *Corros. Sci.* **2017**, *125*, 139–151. [[CrossRef](#)]
23. Solomon, M.M.; Umoren, S.A.; Obot, I.B.; Sorour, A.A.; Gerengi, H. Exploration of Dextran for Application as Corrosion Inhibitor for Steel in Strong Acid Environment: Effect of Molecular Weight, Modification, and Temperature on Efficiency. *ACS Appl. Mater. Interfaces* **2018**, *10*, 28112–28129. [[CrossRef](#)]
24. Thongchaiwetcharat, K.; Jenjob, R.; Seidi, F.; Crespy, D. Programming pH-responsive release of two payloads from dextran-based nanocapsules. *Carbohydr. Polym.* **2019**, *217*, 217–223. [[CrossRef](#)]
25. Zhang, Q.H.; Xu, N. Developing two amino acid derivatives as high-efficient corrosion inhibitors for carbon steel in the CO₂-containing environment. *Ind. Crops Prod.* **2023**, *201*, 116883. [[CrossRef](#)]
26. Chen, J.; Li, J.; Li, B. Identification of molecular driving forces involved in the gelation of konjac glucomannan: Effect of degree of deacetylation on hydrophobic association. *Carbohydr. Polym.* **2011**, *86*, 865–871. [[CrossRef](#)]
27. Liu, W.; Hu, C.; Liu, Y.; Dai, S.; Lu, W.; Lv, X.; Yao, W.; Gao, X. Preparation, characterization, and α -glycosidase inhibition activity of a carboxymethylated polysaccharide from the residue of *Sarcandra glabra* (Thunb.) Nakai. *Int. J. Biol. Macromol.* **2017**, *99*, 454–464. [[CrossRef](#)]
28. Xie, L.; Shen, M.; Wang, Z.; Xie, J. Structure, function and food applications of carboxymethylated polysaccharides: A comprehensive review. *Trends Food Sci. Technol.* **2021**, *118*, 539–557. [[CrossRef](#)]
29. Umoren, S.A.; Solomon, M.M.; Saji, V.S. (Eds.) Chapter 6—Chitosan derivatives. In *Polymeric Materials in Corrosion Inhibition*; Elsevier: Amsterdam, The Netherlands, 2022; pp. 155–185.
30. Zhang, Q.H.; Hou, B.S.; Li, Y.Y.; Zhu, G.Y.; Lei, Y.; Wang, X.; Liu, H.F.; Zhang, G.A. Dextran derivatives as highly efficient green corrosion inhibitors for carbon steel in CO₂-saturated oilfield produced water: Experimental and theoretical approaches. *Chem. Eng. J.* **2021**, *424*, 130519. [[CrossRef](#)]
31. Ren, J.-L.; Sun, R.-C.; Peng, F. Carboxymethylation of hemicelluloses isolated from sugarcane bagasse. *Polym. Degrad. Stab.* **2008**, *93*, 786–793. [[CrossRef](#)]
32. Chaubey, N.; Savita; Qurashi, A.; Chauhan, D.S.; Qurashi, M.A. Frontiers and advances in green and sustainable inhibitors for corrosion applications: A critical review. *J. Mol. Liq.* **2021**, *321*, 114385. [[CrossRef](#)]
33. Fan, L.; Wang, L.; Gao, S.; Wu, P.; Li, M.; Xie, W.; Liu, S.; Wang, W. Synthesis, characterization and properties of carboxymethyl kappa carrageenan. *Carbohydr. Polym.* **2011**, *86*, 1167–1174. [[CrossRef](#)]

34. Xu, P.; Fu, Q.; Zhao, M. The influence of calcium on copper corrosion and its by-product release in drinking water. *RSC Adv.* **2023**, *13*, 17842–17855. [[CrossRef](#)] [[PubMed](#)]
35. Číhal, V.R.; Štefec, R. On the development of the electrochemical potentiokinetic method. *Electrochim. Acta* **2001**, *46*, 3867–3877. [[CrossRef](#)]
36. Chen, S.; Chen, H.; Tian, J.; Wang, Y.; Xing, L.; Wang, J. Chemical modification, antioxidant and α -amylase inhibitory activities of corn silk polysaccharides. *Carbohydr. Polym.* **2013**, *98*, 428–437. [[CrossRef](#)] [[PubMed](#)]
37. Li, J.; Chen, Z.; Shi, H.; Yu, J.; Huang, G.; Huang, H. Ultrasound-assisted extraction and properties of polysaccharide from Ginkgo biloba leaves. *Ultrason. Sonochem.* **2023**, *93*, 106295. [[CrossRef](#)] [[PubMed](#)]
38. Tang, Z.; Huang, G.; Huang, H. Ultrasonic/cellulase-assisted extraction of polysaccharide from Garcinia mangostana rinds and its carboxymethylated derivative. *Ultrason. Sonochem.* **2023**, *99*, 106571. [[CrossRef](#)]
39. Luo, Z.-G.; Zhang, Y.; Wang, H.; Wan, S.; Song, L.-F.; Liao, B.-K.; Guo, X.-P. Modified nano-lignin as a novel biomass-derived corrosion inhibitor for enhanced corrosion resistance of carbon steel. *Corros. Sci.* **2024**, *227*, 111705. [[CrossRef](#)]
40. Rbaa, M.; Benhiba, F.; Hssissou, R.; Lakhri, Y.; Lakhri, B.; Touhami, M.E.; Warad, I.; Zarrouk, A. Green synthesis of novel carbohydrate polymer chitosan oligosaccharide grafted on d-glucose derivative as bio-based corrosion inhibitor. *J. Mol. Liq.* **2021**, *322*, 114549. [[CrossRef](#)]
41. Jin, J.; Wu, G.; Zhang, Z.; Guan, Y. Effect of extracellular polymeric substances on corrosion of cast iron in the reclaimed wastewater. *Bioresour. Technol.* **2014**, *165*, 162–165. [[CrossRef](#)]
42. Abd El-Lateef, H.M.; Gouda, M.; Shalabi, K.; Al-Omair, M.A.; Khalaf, M.M. Superhydrophobic films-based nonanyl carboxy methylcellulose grafted polyacrylamide for AISI-stainless steel corrosion protection: Empirical explorations and computational models. *J. Mol. Liq.* **2022**, *356*, 119063. [[CrossRef](#)]
43. Verma, C.; Hussain, C.M. 10—Chitosan and its derivatives as environmental benign corrosion inhibitors: Recent advancements. In *Environmentally Sustainable Corrosion Inhibitors*; Hussain, C.M., Verma, C., Aslam, J., Eds.; Elsevier: Amsterdam, The Netherlands, 2022; pp. 205–217.
44. Wei, G.; Deng, S.; Xu, D.; Xu, J.; Shao, D.; Li, X. Invasive weed of Eupatorium Adenophora Spreng leaves extract as a novel efficient inhibitor for the corrosion of cold rolled steel in chloroacetic acid solution. *J. Mol. Liq.* **2024**, *400*, 124501. [[CrossRef](#)]
45. Wang, C.; Gao, X.; Chen, Z.; Chen, Y.; Chen, H. Preparation, Characterization and Application of Polysaccharide-Based Metallic Nanoparticles: A Review. *Polymers* **2017**, *9*, 689. [[CrossRef](#)] [[PubMed](#)]
46. Ramezanzadeh, M.; Bahlakeh, G.; Ramezanzadeh, B. Elucidating detailed experimental and fundamental understandings concerning the green organic-inorganic corrosion inhibiting molecules onto steel in chloride solution. *J. Mol. Liq.* **2019**, *290*, 111212. [[CrossRef](#)]
47. Jero, D.; Caussé, N.; Marsan, O.; Buffeteau, T.; Chaussec, F.; Buvignier, A.; Roy, M.; Pébère, N. Film-forming amines adsorption and corrosion kinetics on carbon steel surface in neutral solution investigated by EIS and PM-IRRAS analysis. *Electrochim. Acta* **2023**, *443*, 141925. [[CrossRef](#)]
48. Liu, H.; Xu, L.; Zeng, J. Role of corrosion products in biofilms in microbiologically induced corrosion of carbon steel. *Br. Corros. J.* **2013**, *35*, 131–135. [[CrossRef](#)]
49. Tian, H.; Cui, Z.; Zhang, X.; Zhang, X. Effect of cathodic potential and corrosion product on tribocorrosion behavior of S420 steel in the marine environment. *Mater. Today Commun.* **2024**, *38*, 108372. [[CrossRef](#)]
50. Wang, J.; Ma, L.; Ding, X.; Xu, H.; Wang, Y.; Zhao, M.; Ren, C.; Zhang, D. Tea polyphenol radical scavenger loaded UV absorber for corrosion resistant and weathering resistant epoxy coating fabrication. *Prog. Org. Coat.* **2023**, *180*, 107553. [[CrossRef](#)]
51. Scarcello, E.; Herpain, A.; Tomatis, M.; Turci, F.; Jacques, P.J.; Lison, D. Hydroxyl radicals and oxidative stress: The dark side of Fe corrosion. *Colloids Surf. B Biointerfaces* **2020**, *185*, 110542. [[CrossRef](#)] [[PubMed](#)]
52. Vaszilcsin, C.G.; Putz, M.V.; Kellenberger, A.; Dan, M.L. On the evaluation of metal-corrosion inhibitor interactions by adsorption isotherms. *J. Mol. Struct.* **2023**, *1286*, 135643. [[CrossRef](#)]
53. Wang, D.; Gao, L.; Zhang, D.; Yang, D.; Wang, H.; Lin, T. Experimental and theoretical investigation on corrosion inhibition of AA5052 aluminium alloy by l-cysteine in alkaline solution. *Mater. Chem. Phys.* **2016**, *169*, 142–151. [[CrossRef](#)]
54. Kokalj, A. Corrosion inhibitors: Physisorbed or chemisorbed? *Corros. Sci.* **2022**, *196*, 109939. [[CrossRef](#)]
55. Scheerder, J.; Breur, R.; Slaghek, T.; Holtman, W.; Vennik, M.; Ferrari, G. Exopolysaccharides (EPS) as anti-corrosive additives for coatings. *Prog. Org. Coat.* **2012**, *75*, 224–230. [[CrossRef](#)]
56. Bhatia, A.K.; Dewangan, S.; Vaidya, N. Chapter 22—Carbohydrates and derivatives as green corrosion inhibitors. In *Computational Modelling and Simulations for Designing of Corrosion Inhibitors*; Verma, D.K., Verma, C., Aslam, J., Eds.; Elsevier: Amsterdam, The Netherlands, 2023; pp. 435–460.

Disclaimer/Publisher’s Note: The statements, opinions and data contained in all publications are solely those of the individual author(s) and contributor(s) and not of MDPI and/or the editor(s). MDPI and/or the editor(s) disclaim responsibility for any injury to people or property resulting from any ideas, methods, instructions or products referred to in the content.